Published by Avanti Publishers

Journal of Advances in Applied & Computational Mathematics

ISSN (online): 2409-5761

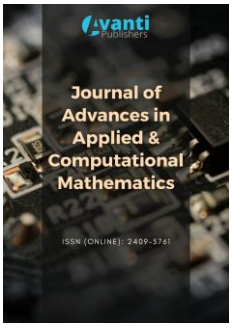

Evidence Theory based Uncertainty Design Optimization for Planetary Gearbox in Wind Turbine

Shiyuan Yang*, Jiapeng Wang and Hengfei Yang

School of Mechanical and Electrical Engineering, University of Electronic Science and Technology of China, Chengdu, 611731, China

ARTICLE INFO

Article Type: Review Article

Keywords:
Optimization
Evidence theory
Interval variables
Random variables
Planetary gearbox

Timeline:
Received: January 24, 2022
Accepted: March 10, 2022
Published: May 24, 2022

Citation: Yang S, Wang J, Yang H. Evidence Theory based Uncertainty Design Optimization for Planetary Gearbox in Wind Turbine. J Adv App Comput Math. 2022; 9: 86-102.

DOI: https://doi.org/10.15377/2409-5761.2022.09.7

ABSTRACT

The planetary gearbox is an important part of the wind turbine. There are many random uncertain factors in the process of design, production, installation, and use, and these uncertain factors greatly influence the service life and reliability of the planetary gearbox. Therefore, the influence of uncertain factors needs to be considered in the design process to reduce the risk of failure. In this paper, an uncertainty design optimization method based on evidence theory is proposed, which can consider both interval variables and random variables in the optimization process. Then the megawatt wind turbine planetary gearbox is taken as the research object to analyze its uncertainty sources. Finally, the planetary gearbox is optimized by the proposed method. By comparing the results, the design scheme obtained by the method proposed in this paper is more reliable.

*Corresponding Author
Email: 13699441285@163.com
Tel: 18848454875

1. Introduction

Wind turbines include drive systems, power generation equipment, and other electromechanical components. Because wind turbines are generally installed in mountains, wilderness, beaches, islands, and other places, and the capacity of wind turbines has gradually increased, it has gradually developed to megawatt-level wind turbines. Therefore, the system structure is also becoming more and more complex, and the probability of failure is increasing [1]. In the drive system of the wind turbine, the planetary gearbox is a crucial component. The wind wheel must transmit the power to the generator through the planetary gearbox gear pair and get the corresponding speed. As a power transmission component, the planetary gearbox is usually installed in a narrow tower space [2]. Once failure occurs, maintenance is difficult and costly. Therefore, the wind power generation system has high requirements on the service life of the planetary gearbox.

At present, scholars have done a lot of research on the design of planetary gearboxes. In the design process, Li *et al*. [3] checked the contact and bending fatigue strengths of the sun gear and planetary gear, respectively, to verify the calculation results. Finally, the designed gearbox is analyzed by modeling and finite element analysis methods. Yang *et al*. [4] calculated the forces acting on the pitch circles of planetary gears, as well as the forces and lifetimes of planetary bearings in a two-stage planetary transmission. Then, the obtained results were compared with a single rotor wind turbine. Chen *et al*. [5] developed a dynamic model of a planetary gearbox considering the clearances of the planetary gear, sun gear, and load-bearing as well as the crack level of the sun gear teeth, which laid the foundation for the reliability design of the planetary gearbox.

The inherent reliability of planetary gearboxes is determined by the design, manufacture, and production process [6,7]. The reliability of use shown in its working process is affected by many factors, including the accuracy of parts manufacturing, machining and assembly, changes in wind load, temperature changes on material properties and lubrication properties, corrosive gases and other factors [8-10]. Most of these factors are difficult to quantify. Usually users focus on the reliability of planetary gearboxes during use. However, to improve its reliability during use, in addition to regular and proper maintenance, it is more important to fully consider the influence of uncertain factors in the design stage. Therefore, it is of great significance to study the reliability of planetary gearboxes under different working conditions and to improve the reliability indicators in its design [11].

However, by introducing reliability into the design, although it can guarantee or predict the probability that the designed product will complete the specified function under the specified conditions of use and within the specified use time, it cannot guarantee that the product has the best operating performance and the lowest cost. Therefore, in order to make the planetary gearbox meet not only the reliability requirements but also have the optimal design results, which is necessary to combine the reliability design theory with the optimization design technology. This is the reliability optimization design method. According to this design method, not only the reliability of the planetary gearbox in use can be given quantitatively, but also the optimal solution of the planetary gearbox in terms of function, parameter matching, structure size, and quality can be obtained.

However, in the optimal design method, dealing with uncertain factors is a difficult problem at present. Schietzold *et al*. [12] propose a framework for considering polymorphic uncertain priors and design parameters in multi-objective optimization. Based on this framework, parameter-based geometric design optimization of steel hooks is studied. Ding [13] devised a general simulation algorithm to estimate uncertain random expected values. In the optimization process, Mourelatos [14] proposes an optimal design method based on evidence theory that only considers interval variables.

However, the above studies only consider the impact of objective uncertainty or cognitive uncertainty. Aiming at the above problems, this paper proposes a method using interval and random mixed variables to describe design variables and parameters with subjective and objective uncertainties. Then use evidence theory to carry out the reliability optimization design under interval and random mixed variables so as to obtain the optimal design solution considering interval and random uncertainty. The core idea of this method is divided into the following steps: First, in the interval segment, the extreme value of the limit state function is estimated by the

vertex method. Then, the reliability extrema of the limit state function are estimated at the extreme point using the First Order Reliability Method (FORM) [15]. Finally, the optimal design is carried out using the Evidence-Based Design Optimization (EBDO) algorithm that only considers interval variables.

The other parts of this paper are organized as follows. In Section 2, the basic content of evidence theory is introduced. In Section 3, the EBDO method that considers both interval variables and random variables are proposed. The mathematical model of this method is further given. In Section 4, the proposed method is applied to the optimal design of the planetary gearbox for megawatt wind turbines, and the optimal mathematical model is given. In Section 5, the optimization results of the proposed method on the research object are analyzed, and the proposed method is proved to be feasible. Finally, Section 6 concludes the paper.

2. The Basic Content of Evidence Theory

Evidence theory is also known as D-S theory. The D-S theory was proposed by the scholar Dempster in the mid-twentieth century [16]. As a student of Dempster, Shafer further generalized, theorized, and systematized evidence theory. Since its birth, the D-S theory has gradually become one of the research hotspots. The research on the theory of evidence is mainly divided into two aspects: one is the perfection and development of its own theory; the other is the research on the extension and application of the theory of evidence. So that evidence theory can be better applied to practical engineering.

This part will briefly introduce the basic content of evidence theory. Ref. [16-18] introduces the optimal design and fuzzy calculation process of evidence theory in detail.

If a proposition is solved based on the theory of evidence, its purpose is to transform the processing of a proposition into solving a set. The basis for this transformation is the identification frame. Suppose Θ is a finite non-empty orthogonal set (space), called the identification space. Every possible hypothesis is included in this space.

$$\Theta = \{Interval_1, Interval_2, \cdots, Interval_m\}. \tag{1}$$

where: $Interval_i$ is a value range of the interval variable.

The power set of the identification frame contains all possible propositions formed by the basic propositions in Θ through "and", "not", "or" and other logical relations, the number of which is 2^n, denoted by 2^Θ.

After the identification framework is determined, the credibility is reset to the assignment based on the evidence. That is, researchers further interpret and analyze the evidence to ensure that the evidence can reliably support any proposition. This process is called Basic Probability Assignments (BPA), which is similar to the probability density function in probability theory. BPA function $m: 2^\Theta \to [0,1]$, $m(\cdot) \in [0,1]$.It satisfies:

$$m(X) \geq 0, \forall \in 2^\Theta \tag{2}$$

$$m(\Phi) = 0 \tag{3}$$

$$\sum_{X \subseteq \Theta} m(X) = 1 \tag{4}$$

where: m is the basic credibility distribution function; X is any subset of the power set 2^Θ corresponding to the recognition frame; $m(X)$ is the credibility number of the event X; the interval X of $m(X) \geq 0$ is called the focal element.

When the BPAs of each possibility in the set Θ are known, the Belief measure (Bel) and the Plausibility measure (Pl) of X can be calculated by Eq. (5).

$$\begin{cases} Bel(X) = \sum_{Y \subseteq X} m(Y), & X \subseteq \Theta \\ Pl(X) = \sum_{Y \cap X \neq \Phi} m(Y), & X \subseteq \Theta, Y \subseteq \Theta \end{cases} \tag{5}$$

where: $m(Y)$ is the credibility number of the event Y.$Bel(X)$ is the sum of the BPAs of the focal elements fully contained by the proposition X, and $Pl(X)$ is the sum of the BPAs of the focal elements that intersect with the proposition X.

Evidence theory is a fuzzy calculation method based on Bel and Pl, and imprecision or uncertainty can be represented by Bel and Pl [19]. In the Dempster-Shafer (D-S) evidence theory, the Bel of X is the minimum possibility of X, and the Pl of X is the maximum possibility of X, so there is the following relationship:

$$\begin{cases} Pl(X) = 1 - Bel(\bar{X}) \\ Pl(X) \geq Bel(X) \end{cases} \tag{6}$$

When evidence comes from different independent sources or different experts, even if the evidence obtained is contradictory, D-S evidence theory can also be merged. Assuming that A and B are BPAs with evidence from two different independent sources or experts, they can be fused as follows [20]:

$$m(X) = m_1(Y) \oplus m_2(Z) = \begin{cases} 0, & Y \cap Z = \emptyset \\ \frac{\sum_{Y \cap Z = X} m_1(Y) \times m_2(Z)}{1 - \sum_{Y \cap Z = \emptyset} m_1(Y) \times m_2(Z)}, & Y \cap Z \neq \emptyset \end{cases} \tag{7}$$

Where: $\sum_{Y \cap Z = \emptyset} m_1(Y) \times m_2(Z)$ addresses the degree of conflict in evidence from disparate sources of information. The larger the value, the more severe the conflict between the information.

3. EBDO Considering Both Interval Variables and Random Variables

At present, the optimal design method based on evidence theory only considers interval variables. It discretely divides random variables that conform to specific probability distributions according to their probability density functions but do not reasonably and effectively apply known information to the discretization of random variables, making it possible to optimize the results further. This paper improves the optimal design method based on evidence theory [16,17]. Both interval and random variables are considered in the optimization process. In the reliability analysis, the extreme point of the limit state function is analyzed first, and then the FORM is used to analyze the reliability of the limit state function in the reliability analysis [15]. When carrying out the optimal design, the improved EBDO is applied to carry out the optimal design.

3.1. Estimation of Extremum Reliability of Limit State Function with Interval Random Mixed Variables

The reliability can be understood as the probability that the limit state function $g(X) \geq 0$ is caused by the uncertainty factor after the optimization design average point is determined. Therefore, when the limit state function$g(X) \geq 0$ the farther the mean point of the optimized design is from the constraint boundary, the higher the calculated reliability; conversely, when the limit state function$g(X) \leq 0$, the farther the mean point of the optimized design is from the constraint boundary, the lower the calculated reliability is also. From the above analysis, when the limit state function includes interval variables and random variables, and the mean value, the variance of the random variable, and the upper and lower boundaries of the interval variable are known, the reliability limit value of the limit state function in a certain interval can be calculated by Eq. (8).

$$R = [P(min(\, g(c_j), g(E_k)) \geq 0), P(max(\, g(c_j), g(E_k)) \geq 0)] \; j = 1,2, \cdots N, k = 1,2, \cdots, m \tag{8}$$

where: E_k represents the kth extreme point except the extreme boundary point; m represents the number of extreme points other than the extreme boundary point. FORM is used to calculate the reliability.

3.2. The Calculation of Bel and Pl in Reliability Analysis Considering Interval Variables and Random Variables

In this paper, the Bel and Pl in reliability analysis considering interval variables and random variables are calculated by using the transformation function [21].

$$P = Pr\{G(Y,X) \geq 0\} \tag{9}$$

where: Y is the interval variable vector; X is the random variable vector; $G(\cdot)$is the limit state function; $Pr\{\cdot\}$represents the probability value when$g(\cdot) \geq 0$.

Assuming that y_{set1} and y_{set2} $(y_{set1} \in Y, y_{set2} \in Y)$ are two independent interval variables, and their BPAs are the values after fusion of D-S evidence theory. Define the vector $c_{ij} = [y_{set1i}, y_{set2j}]$.

$$C = y_{set1} \times y_{set2} = \{c_{ij} = [y_{set1i}, y_{set2j}], y_{set1i} \in y_{set1}, y_{set2i} \in y_{set2},\} \tag{10}$$

where: C represents the combined interval, and N^1, N^2 $(i \in N^1, j \in N^2)$ is the interval variable number of y_{set1} and y_{set2}, respectively. Because all variables are independent of each other, the BPAs of C can be calculated by Eq. (11).

$$m_c(h_{ij}) = m(y_{set1i})m(y_{set2j}), \quad \sum_{i,j} m_c(h_{ij}) = 1 \tag{11}$$

Define an interval function *F*:

$$F = \{g_{ij}: g_{ij} = Pr_{ij}\{G(Y,X) \geq 0\}, i \in N^1, j \in N^2\} \tag{12}$$

where: $Pr_{ij}\{\cdot\}$ represents the probability value of $y_1 \in y_{set1i}, y_2 \in y_{set2i}$.

Because Y is an interval variable vector and X is a random variable vector, g_{ij} is an interval value, and the following equation can calculate its maximum and minimum values:

$$\left[gij\_max_{ij\_min} = [Pr_{ij\_worst} - Pr_0, Pr_{ij\_best} - Pr_0,]\right] \tag{13}$$

Where: Pr_{ij_worst} is the minimum probability value of $y \in c_{ij}$; Pr_{ij_best} is the maximum probability value of $y \in c_{ij}$; Pr_{ij_worst} and .Pr_{ij_best} can be calculated by Eq. (9).

The calculation relationship between Bel and Pl is shown in Fig. **1**:

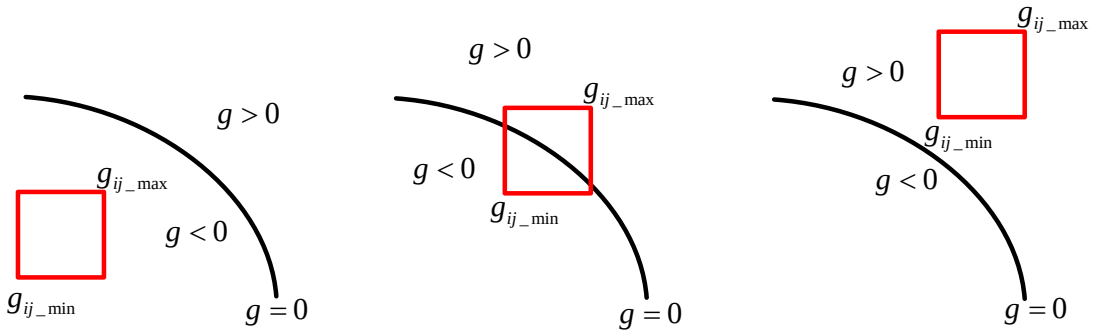

Figure 1: The calculation relationship between Bel and Pl.

When $y \in c = [y_{set1i}, y_{set2j}]$ is $y_1 \in [y_{set1i\_l}, y_{set1i\_u}]$, $y_2 \in [y_{set2i\_l}, y_{set2i\_u}]$, if g_{ij_min}, g_{ij_max}, then $m_c(h_{ij}) \notin Bel(F)$, $m_c(h_{ij}) \notin Pl(F)$; if g_{ij_min}, g_{ij_max}, then $m_c(h_{ij}) \notin Bel(F)$, $m_c(h_{ij}) \in Pl(F)$; if g_{ij_min}, g_{ij_max}, then $m_c(h_{ij}) \in Bel(F)$, $m_c(h_{ij}) \in Pl(F)$. From the above analysis, there are the following relationships:

$$Bel(F) \le P \le Pl(F) \tag{14}$$

where: $P = Pr(G \ge 0)$ is the true probability value of *F*.

3.3. The Mathematical Model of EBDO Considering Interval Variable and Random Variable Simultaneously

Because of $Bel(g \ge 0) \le P(g \ge 0) \le Pl(g \ge 0)$, the following relation can be obtained from Eq. (14).

$$\begin{cases} \text{if } Bel(g \ge 0) \ge R, \text{then } P(g \ge 0) \ge R \\ \text{if } Pl(g \le 0) \le P_f, then \ P(g \le 0) \ge P_f \end{cases} \tag{15}$$

where: R is the probability value when feasible and $P_f = 1 - R$ is the probability value when it fails.

The EBDO model considering both interval and random variables can be expressed as follows:

$$\begin{aligned} &\min_{\mathrm{d,X,Y}} \quad f(\mathrm{d},\mathrm{X}^N,\mathrm{Y}^I,P^N,P^I) \\ &\text{s.t.} \quad Bel(Pr_{worst}\{g_i(\mathrm{d},\mathrm{X}^N,\mathrm{Y}^I,P^N,P^I) \ge 0\} - P_{r0i} > 0) \ge R_i, \qquad i = 1,2,\cdots,n \\ &\quad d^L \le d \le d^U, X^L \le X \le X^U, Y^L \le Y \le Y^U \end{aligned} \tag{16}$$

Where: d is the deterministic design variable vector, X^N is the random design variable vector, Y^I is the interval design variable vector, P^N is the random design parameter vector, P^I is the interval design parameter vector, $f(\cdot)$is the objective function, $g(\cdot)$is the limit state function, n is the number of constraint functions.

The algorithm flow of EBDO considering interval and random variables is shown in Fig. **2**:

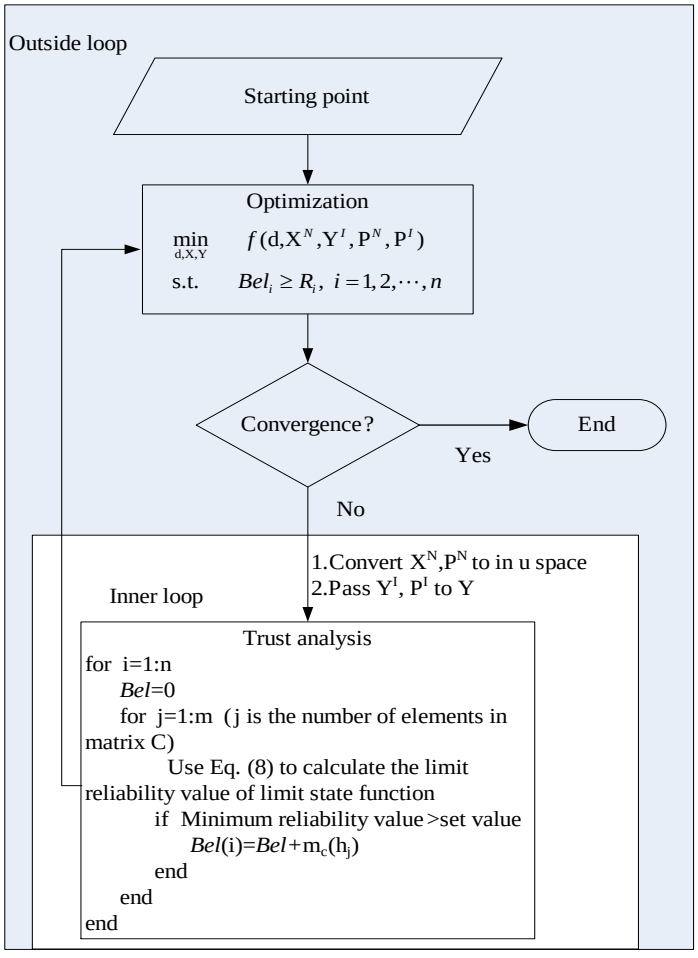

Figure 2: Flow chart of EBDO algorithm considering interval and random variables.

4. EBDO Optimization Mathematical Model of Planetary Gearbox for Megawatt Wind Turbine

4.1. Overview of 1.5 MW Wind Turbine Planetary Gearbox Structure

The real structure diagram of the planetary gearbox is shown in Fig. **3**. Because the rated input speed of the planetary gearbox does not exceed 20 r/min and the output speed is above 1790 r/min [22], the 1.5MW wind turbine planetary gearbox is connected with a 2-stage parallel shaft and a 1-stage planetary transmission structure, as shown in Fig. **4**.

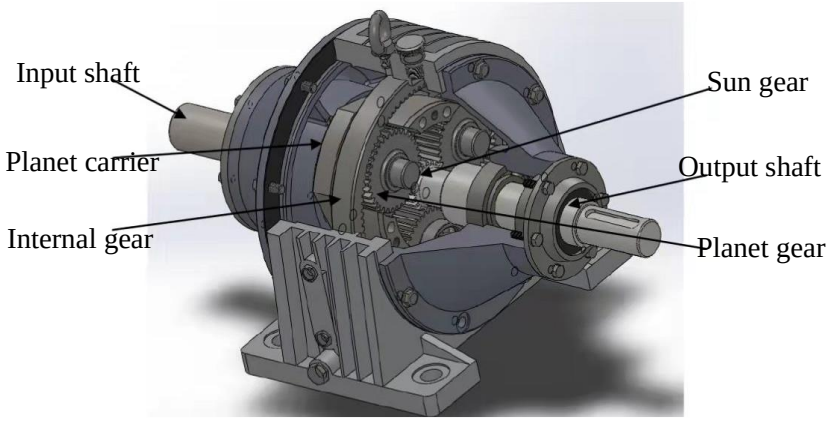

Figure 3: Real structure diagram of planetary gearbox.

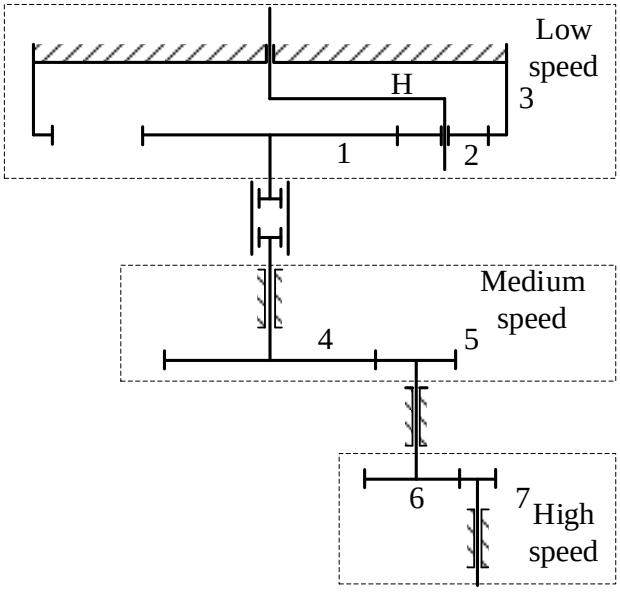

Figure 4: Schematic diagram of 1.5MW wind turbine planetary gearbox structure [23].

In Fig. **4**, 1 represents the sun gear in the planetary gear train; 2 represents the planetary gear in the planetary gear train; 3 represents the fixed ring gear in the planetary gear train; H represents the planet carrier in the planetary gear train. Both the intermediate stage and the high-speed stage are driven by helical gears, 4 and 5 represent the intermediate stage gears, and 6 and 7 represent the high-speed stage gears. Compared with the spur gear, the helical gear increases the total contact area of the gear pair, which can increase the bearing capacity of the speed increase box, improve the stability of the output shaft end of the speed increaser, and increase the stability of rotation. Therefore, the gears in the planetary gearbox use helical gears.

4.2. Uncertainty Source Analysis in Optimization Design of Planetary Gearbox for Wind Turbine

Wind turbines are commonly installed in mountains, wilderness, beaches, and islands [24]. They are often affected by irregularly variable loads and strong gusts of wind. These environmental factors are subject to great uncertainty [25]. The planetary gearbox is a key component of the wind turbine drive system. The wind wheel must transmit the power to the generator through the planetary gearbox so that it can get the corresponding speed. As a part of power transmission, planetary gearboxes have great uncertainty in the dynamic and static loads during operation [26].

There are many objective uncertainties in the machining process of planetary gearboxes, such as random errors in machining dimensions and random non-uniformity of material properties. There is also an installation error in the installation of the planetary gearbox. If these uncertainties are not considered in the design of the planetary gearbox, there will be unpredictable consequences for the reliability of the wind power system

Due to the lack of design methods, design means, and knowledge, the final design of the planetary gearbox is likely to be quite different from the real needs. This is also the uncertainty in the design process.

Most of the above-mentioned uncertainty factors are difficult to describe with specific probability distributions, and EBDO considering interval variables and random variables can deal with the uncertainties in the optimization design process at the same time. Therefore, the optimal design of the planetary gearbox will be carried out using EBDO considering multi-interval variables and random variables.

4.3. The Embodiment of Uncertainty in the Optimization Design Process of Wind Turbine Planetary Gearbox

In the initial stage of optimization design of planetary gearbox for the wind turbine, the actual uncertainties are mainly reflected in the interval variables and random variables in the design process. This paper discusses how to optimize the design of the planetary gearbox of the megawatt wind turbine. All the gears used in the gearbox are helical, so the optimization design of the nine helical gear parameters in the gearbox is the design focus of this paper.

The independent parameters selected and determined in the design process are called design variables [27], and the design variables include continuous design variables and discrete design variables. In this paper, the design variables are the number of helical gear teeth Z, the normal modulus m_n, the helix angle β, and the tooth width coefficient ϕ_d. In the optimization design of this paper, the normal displacement coefficient A of the helical gear is not regarded as a design variable. The data in the helical gear of the wind turbine planetary gearbox will be determined according to the final optimized result, the strength requirements of the helical gear, and the original design scheme.

In the process of optimal design, in addition to the parameters used as design variables, the parameters whose value fluctuates are called uncertain design parameters. In this design, the uncertain design parameters include environment-related parameters, manufacturing process-related parameters, and material-related parameters. There is a certain deviation between the theoretical and actual values of these parameters. Some of these deviations can be expressed by specific probability distributions. Some can only be expressed in a certain probability interval.

Therefore, there are 10 parameters involved in this design ($K_A, K_V, K_{\mathrm{H}\beta}, K_{\mathrm{F}\beta}, K_{H\alpha}, K_{F\alpha}, K_{\mathrm{HP}}, K_{\mathrm{FP}}, Y_{\mathrm{FS}}, \sigma_{\mathrm{HP}}, \sigma_{\mathrm{FP}}, P, n$). K_A and K_V are the service factor and dynamic load factor, respectively; $K_{\mathrm{H}\beta}$ and $K_{\mathrm{F}\beta}$ are the tooth load distribution coefficients; $K_{H\alpha}$ and $K_{F\alpha}$ are the load distribution coefficients between teeth; K_{HP} and K_{FP} are the transmission load non-uniformity coefficients of NGW type planetary gears; Y_{FS} is compound tooth shape coefficients; σ_{HP} and σ_{FP} are the allowable stress of the tooth surface contact fatigue and the allowable stress of the tooth root bending fatigue of the helical gear, respectively; P and n are the input power and speed, respectively.

The parameter selection and value selection in the optimization design process in this paper mainly refer to Ref. [28-30].

4.4. Optimization Mathematical Model of EBDO for Planetary Gearbox of Wind Turbine Considering Interval Variables and Random Variables

4.4.1. Selection of Design Variables

Considering the convenience of optimization calculation, this paper regards the number of teeth as a continuous variable. Then round off the result. However, rounding results tend to invalidate the constraints of the limit state function, which is sometimes very dangerous when designing. Here, in order to solve the failure problem that may be caused by rounding, this paper adopts the following solutions. First, when calculating the maximum and minimum reliability values of the corresponding limit state function, calculate the limit reliability value of the change of the number of teeth within the interval of Eq. (17). Then the calculated limit value is used to calculate the corresponding limit state function confidence and likelihood.

$$z \in [z - mod(z,1), z - mod(z,1) + 1] \tag{17}$$

where: z is the number of teeth; $mod(z,1)$ is the remainder of z.

The comprehensive analysis shows that in the case of the total speed-up ratio $i = \frac{1}{88.8}$, only the characteristics of the helical gears 1, 4, and 6 greatly influence the design of the 1.5MW wind turbine planetary gearbox. These characteristics are the number of teeth z and normal modulus m_n, helix angle β, and tooth face width coefficientϕ_d. A pair of mutually meshing helical gears have the same normal modulus m_n, helix angle β, and tooth face width coefficientϕ_d. Therefore, there are 14 design variables in this design.

$$\begin{aligned} X &= [z_1, z_4, z_6, m_{\mathrm{n}123}, m_{\mathrm{n}45}, m_{\mathrm{n}67}, \beta_{123}, \beta_{45}, \beta_{67}, \phi_{\mathrm{d}123}, \phi_{\mathrm{d}45}, \phi_{\mathrm{d}67}, i_{45}, i_{67}]^T \\ &= [x_1, x_2, x_3, x_4, x_5, x_6, x_7, x_8, x_9, x_{10}, x_{11}, x_{12}, x_{13}, x_{14}]^T \end{aligned} \tag{18}$$

where: z_1 is the number of teeth of sun gear 1; z_4 is the number of teeth of helical gear 4; z_6 is the number of teeth of helical gear 6. $m_{\mathrm{n}123}$, β_{123} and $\phi_{\mathrm{d}123}$ are the normal modulus, helix angle, and tooth face width coefficient of the low-speed helical gear, respectively. $m_{\mathrm{n}45}$, β_{45}, $\phi_{\mathrm{d}45}$ and i_{45} are the normal modulus, helix angle, tooth face width coefficient, and transmission ratio of the intermediate stage helical gear, respectively. $m_{\mathrm{n}67}$, β_{67}, $\phi_{\mathrm{d}67}$ and i_{67} are the normal modulus, helix angle, tooth face width coefficient, and transmission ratio of the intermediate helical gear, respectively.

z_1, z_4, z_6, $m_{\mathrm{n}123}$, $m_{\mathrm{n}45}$, and $m_{\mathrm{n}67}$ are treated as continuous variables when the corresponding optimization program is written. i_{45} and i_{67} are two deterministic design variables. β_{123}, β_{45}, β_{67}, $\phi_{\mathrm{d}123}$, $\phi_{\mathrm{d}45}$, and $\phi_{\mathrm{d}67}$ are random variables treated as fluctuations that conform to a normal distribution.

$$\begin{cases} \beta_{123} \sim N(\beta_{123}, 0.01) \\ \beta_{45} \sim N(\beta_{45}, 0.01) \\ \beta_{67} \sim N(\beta_{67}, 0.01) \\ \phi_{\mathrm{d}123} \sim N(\phi_{\mathrm{d}123}, 0.01) \\ \phi_{\mathrm{d}45} \sim N(\phi_{\mathrm{d}45}, 0.01) \\ \phi_{\mathrm{d}67} \sim N(\phi_{\mathrm{d}67}, 0.01) \end{cases} \tag{19}$$

4.4.2. The Establishment of the Objective Function

Since the planetary gearbox is usually installed in a small space on the top of the tower, when optimizing the design, the volume of the planetary gearbox is as small as possible. At the same time, reducing the volume of the planetary gearbox is beneficial to reduce the mass of the planetary gearbox and thus reduce the production cost. Therefore, this paper takes the volume of the planetary gearbox as the evaluation function. The goal of optimization is to minimize the volume of the planetary gearbox.

The size of the helical gear and the gear shaft is the original basis for determining the size of the planetary gearbox assembly. Therefore, the objective function is established with the volume of the helical gear, regardless of the volume of the planetary gearbox housing and bearing. So far, the volume V of the planetary gearbox can be expressed as a function of the design variables above:

$$\begin{aligned} V &= f(z_1, z_4, z_6, m_{\mathrm{n}123}, m_{\mathrm{n}45}, m_{\mathrm{n}67}, \beta_{123}, \beta_{45}, \beta_{67}, \phi_{\mathrm{d}123}, \phi_{\mathrm{d}45}, \phi_{\mathrm{d}67}, i_{45}, i_{67}) \\ &= \frac{\pi}{4}\left(\frac{m_{\mathrm{n}123} z_1}{cos\,\beta_{123}}\right)^3 \cdot \left(\frac{i_{45} \cdot i_{67}}{i} - 1\right)^2 \cdot \phi_{\mathrm{d}123} + \frac{\pi}{4}\left(\frac{m_{\mathrm{n}45} z_4}{cos\,\beta_{45}}\right)^3 \cdot (1 + i_{45}^2) \cdot i_{45} \cdot \phi_{\mathrm{d}45} \\ &\quad + \frac{\pi}{4}\left(\frac{m_{\mathrm{n}67} z_6}{cos\,\beta_{67}}\right)^3 \cdot (1 + i_{67}^2) \cdot i_{67} \cdot \phi_{\mathrm{d}67} \end{aligned} \tag{20}$$

where: the meanings of $z_1, z_4, z_6, m_{\mathrm{n}123}, m_{\mathrm{n}45}, m_{\mathrm{n}67}, \beta_{123}, \beta_{45}, \beta_{67}, \phi_{\mathrm{d}123}, \phi_{\mathrm{d}45}, \phi_{\mathrm{d}67}, i_{45}$ and i_{67} are explained in 4.4.1.

Since the design variables in this paper include interval variables and random variables, and the design parameters include interval parameters and random parameters, the objective function is expressed as:

$$\begin{aligned} f &= f(\mathrm{X},\mathrm{X}^N,\mathrm{Y}^I,\mathrm{P}^N,\mathrm{P}^I)\frac{\pi}{4}\left(\frac{x_4 x_1}{cos\,x_7}\right)^3 \cdot \left(\frac{x_{13} x_{14}}{i} - 1\right)^2 \cdot x_{10} + \frac{\pi}{4}\left(\frac{x_5 x_2}{cos\,x_8}\right)^3 \cdot (1 + x_{13}^2) \cdot x_{13} \cdot x_{11} \\ &+ \frac{\pi}{4}\left(\frac{x_6 x_3}{cos\,x_9}\right)^3 \cdot (1 + x_{14}^2) \cdot x_{14} \cdot x_{12} \end{aligned} \tag{21}$$

Where: X is a deterministic design variable, in this design $\mathrm{X}=[i_{45}, i_{67}] = [x_{13}, x_{14}]$; X^N is a random design variable, in this design $X^N = [\beta_{123}, \beta_{45}, \beta_{67}, \phi_{\mathrm{d}123}, \phi_{\mathrm{d}45}, \phi_{\mathrm{d}67}] = [x_7, x_8, x_9, x_{10}, x_{11}, x_{12}]$; Y^I is an interval design variable, in this design $Y^I = [z_1, z_4, z_6, m_{\mathrm{n}123}, m_{\mathrm{n}45}, m_{\mathrm{n}67}] = [x_1, x_2, x_3, x_4, x_5, x_6]$; P^N is a random design parameter, $P^N = [K_A, K_V, K_{\mathrm{H}\beta}, K_{\mathrm{F}\beta}, K_{H\alpha}, K_{F\alpha}, K_{\mathrm{HP}}, K_{\mathrm{FP}}, Y_{\mathrm{FS}}, \sigma_{\mathrm{HP}}, \sigma_{\mathrm{FP}}]$; P^I is an interval design parameter, in this design $P^I = [P, n]$.

4.4.3. Establishment of Constraints

According to the principle that the equivalent number of teeth of the small helical gears meshing with each other is not less than 17, it can be concluded that the constraint conditions that the number of teeth of the helical gear in the optimal design must meet are:

$$\begin{cases} c_1(\mathrm{X},\mathrm{X}^N,\mathrm{Y}^I,\mathrm{P}^N,\mathrm{P}^I) = 0.99 - \mathrm{Pr\_worst}\{g_1(\mathrm{X},\mathrm{X}^N,\mathrm{Y}^I, P^N, P^I) \le 0\} \le 0 \\ c_2(\mathrm{X},\mathrm{X}^N,\mathrm{Y}^I,\mathrm{P}^N,\mathrm{P}^I) = 0.99 - \mathrm{Pr\_worst}\{g_2(\mathrm{X},\mathrm{X}^N,\mathrm{Y}^I, P^N, P^I) \le 0\} \le 0 \\ c_3(\mathrm{X},\mathrm{X}^N,\mathrm{Y}^I,\mathrm{P}^N,\mathrm{P}^I) = 0.99 - \mathrm{Pr\_worst}\{g_3(\mathrm{X},\mathrm{X}^N,\mathrm{Y}^I, P^N, P^I) \le 0\} \le 0 \end{cases} \tag{22}$$

$$g_1(\mathrm{X},\mathrm{X}^N,\mathrm{Y}^I, P^N, P^I) = 17 - \frac{z_1}{cos^3\,\beta_{123}} \tag{23}$$

$$g_2(\mathrm{X},\mathrm{X}^N,\mathrm{Y}^I, P^N, P^I) = 17 - \frac{z_4 i_{45}}{cos^3\,\beta_{45}} \tag{24}$$

$$g_3(\mathrm{X},\mathrm{X}^N,\mathrm{Y}^I, P^N, P^I) = 17 - \frac{z_6 i_{67}}{cos^3\,\beta_{67}} \tag{25}$$

According to the principle that the normal modulus of the helical gear should not be less than 2mm when it is in power transmission, it can be concluded that the constraint conditions that the normal modulus of the helical gear must satisfy in the optimal design are:

$$\begin{cases} c_4(\mathrm{X},\mathrm{X}^N,\mathrm{Y}^I,\mathrm{P}^N,\mathrm{P}^I) = 2 - m_{\mathrm{n}123} \le 0 \\ c_5(\mathrm{X},\mathrm{X}^N,\mathrm{Y}^I,\mathrm{P}^N,\mathrm{P}^I) = 2 - m_{\mathrm{n}45} \le 0 \\ c_6(\mathrm{X},\mathrm{X}^N,\mathrm{Y}^I,\mathrm{P}^N,\mathrm{P}^I) = 2 - m_{\mathrm{n}67} \le 0 \end{cases} \tag{26}$$

According to engineering experience, this paper takes the helix angle of the helical gear $8^\circ \le \beta \le 15^\circ$. Therefore, the constraints of the helix angle in this paper are:

$$\begin{cases} c_7(\mathrm{X},\mathrm{X}^N,\mathrm{Y}^I,\mathrm{P}^N,\mathrm{P}^I) = 0.99 - P_r\{g_4(\mathrm{X},\mathrm{X}^N,\mathrm{Y}^I,P^N,P^I) \le 0\} \le 0 \\ c_8(\mathrm{X},\mathrm{X}^N,\mathrm{Y}^I,\mathrm{P}^N,\mathrm{P}^I) = 0.99 - P_r\{g_5(\mathrm{X},\mathrm{X}^N,\mathrm{Y}^I,P^N,P^I) \le 0\} \le 0 \\ c_9(\mathrm{X},\mathrm{X}^N,\mathrm{Y}^I,\mathrm{P}^N,\mathrm{P}^I) = 0.99 - P_r\{g_6(\mathrm{X},\mathrm{X}^N,\mathrm{Y}^I,P^N,P^I) \le 0\} \le 0 \\ c_{10}(\mathrm{X},\mathrm{X}^N,\mathrm{Y}^I,\mathrm{P}^N,\mathrm{P}^I) = 0.99 - P_r\{g_7(\mathrm{X},\mathrm{X}^N,\mathrm{Y}^I,P^N,P^I) \le 0\} \le 0 \\ c_{11}(\mathrm{X},\mathrm{X}^N,\mathrm{Y}^I,\mathrm{P}^N,\mathrm{P}^I) = 0.99 - P_r\{g_8(\mathrm{X},\mathrm{X}^N,\mathrm{Y}^I,P^N,P^I) \le 0\} \le 0 \\ c_{12}(\mathrm{X},\mathrm{X}^N,\mathrm{Y}^I,\mathrm{P}^N,\mathrm{P}^I) = 0.99 - P_r\{g_9(\mathrm{X},\mathrm{X}^N,\mathrm{Y}^I,P^N,P^I) \le 0\} \le 0 \end{cases} \tag{27}$$

$$g_4(\mathrm{X},\mathrm{X}^N,\mathrm{Y}^I,P^N,P^I) = 8^\circ - \beta_{123} \tag{28}$$

$$g_5(\mathrm{X},\mathrm{X}^N,\mathrm{Y}^I,P^N,P^I) = 8^\circ - \beta_{45} \tag{29}$$

$$g_6(\mathrm{X},\mathrm{X}^N,\mathrm{Y}^I,P^N,P^I) = 8^\circ - \beta_{67} \tag{30}$$

$$g_7(\mathrm{X},\mathrm{X}^N,\mathrm{Y}^I,P^N,P^I) = \beta_{123} - 15^\circ \tag{31}$$

$$g_8(\mathrm{X},\mathrm{X}^N,\mathrm{Y}^I,P^N,P^I) = \beta_{45} - 15^\circ \tag{32}$$

$$g_9(\mathrm{X},\mathrm{X}^N,\mathrm{Y}^I,P^N,P^I) = \beta_{67} - 15^\circ \tag{33}$$

In this paper, the low-speed transmission adopts NGW planetary helical gear rotation. Considering its use environment, take its transmission ratio range as $1/9\sim1/2.7$. Under the condition that the speed increase ratio $i = 1/88.8$ of the planetary gearbox in this paper is constant, the transmission ratio of the planetary transmission stage is $i/(i_{45}i_{67})$. Therefore, the constraints of the transmission ratio in this paper are:

$$\begin{cases} c_{13}(\mathrm{X},\mathrm{X}^N,\mathrm{Y}^I,\mathrm{P}^N,\mathrm{P}^I) = 1.01i_{45} - i_{67} \le 0 \\ c_{14}(\mathrm{X},\mathrm{X}^N,\mathrm{Y}^I,\mathrm{P}^N,\mathrm{P}^I) = i_{67} - 1.05i_{45} \le 0 \\ c_{15}(\mathrm{X},\mathrm{X}^N,\mathrm{Y}^I,\mathrm{P}^N,\mathrm{P}^I) = \frac{1}{9-\frac{i}{(i_{45}\cdot i_{67})}} \le 0 \\ c_{16}(\mathrm{X},\mathrm{X}^N,\mathrm{Y}^I,\mathrm{P}^N,\mathrm{P}^I) = \frac{i}{(i_{45}\cdot i_{67})-\frac{1}{2.7}} \le 0 \end{cases} \tag{34}$$

Considering the use environment and design requirements, the tooth width coefficient ϕ_d of the planetary gear transmission stage is $0.5 \le \phi_d \le 0.7$. Take the tooth width coefficient ϕ_d of the intermediate and high-speed transmissions as $0.7 \le \phi_d \le 1.2$. Therefore, the constraints of the tooth width coefficient in the design of this paper are:

$$\begin{cases} c_{17}(\mathrm{X},\mathrm{X}^N,\mathrm{Y}^I,\mathrm{P}^N,\mathrm{P}^I) = 0.99 - P_r\{g_{10}(\mathrm{X},\mathrm{X}^N,\mathrm{Y}^I,P^N,P^I) \le 0\} \le 0 \\ c_{18}(\mathrm{X},\mathrm{X}^N,\mathrm{Y}^I,\mathrm{P}^N,\mathrm{P}^I) = 0.99 - P_r\{g_{11}(\mathrm{X},\mathrm{X}^N,\mathrm{Y}^I,P^N,P^I) \le 0\} \le 0 \\ c_{19}(\mathrm{X},\mathrm{X}^N,\mathrm{Y}^I,\mathrm{P}^N,\mathrm{P}^I) = 0.99 - P_r\{g_{12}(\mathrm{X},\mathrm{X}^N,\mathrm{Y}^I,P^N,P^I) \le 0\} \le 0 \\ c_{20}(\mathrm{X},\mathrm{X}^N,\mathrm{Y}^I,\mathrm{P}^N,\mathrm{P}^I) = 0.99 - P_r\{g_{13}(\mathrm{X},\mathrm{X}^N,\mathrm{Y}^I,P^N,P^I) \le 0\} \le 0 \\ c_{21}(\mathrm{X},\mathrm{X}^N,\mathrm{Y}^I,\mathrm{P}^N,\mathrm{P}^I) = 0.99 - P_r\{g_{14}(\mathrm{X},\mathrm{X}^N,\mathrm{Y}^I,P^N,P^I) \le 0\} \le 0 \\ c_{22}(\mathrm{X},\mathrm{X}^N,\mathrm{Y}^I,\mathrm{P}^N,\mathrm{P}^I) = 0.99 - P_r\{g_{15}(\mathrm{X},\mathrm{X}^N,\mathrm{Y}^I,P^N,P^I) \le 0\} \le 0 \end{cases} \tag{35}$$

$$g_{10}(\mathrm{X},\mathrm{X}^N,\mathrm{Y}^I,P^N,P^I) = 0.5 - \phi_{\mathrm{d}123} \tag{36}$$

$$g_{11}(\mathrm{X},\mathrm{X}^N,\mathrm{Y}^I,P^N,P^I) = \phi_{\mathrm{d}123} - 0.7 \tag{37}$$

$$g_{12}(\mathrm{X},\mathrm{X}^N,\mathrm{Y}^I,P^N,P^I) = 0.7 - \phi_{\mathrm{d}45} \tag{38}$$

$$g_{13}(\mathrm{X},\mathrm{X}^N,\mathrm{Y}^I,P^N,P^I) = \phi_{\mathrm{d}45} - 1.2 \tag{39}$$

$$g_{14}(\mathrm{X},\mathrm{X}^N,\mathrm{Y}^I,P^N,P^I) = 0.7 - \phi_{\mathrm{d}67} \tag{40}$$

$$g_{15}(\mathrm{X},\mathrm{X}^N,\mathrm{Y}^I,P^N,P^I) = \phi_{\mathrm{d}67} - 1.2 \tag{41}$$

This paper adopts helical gear transmission. The coincidence degree ε_r of the helical gears meshing with each other is the sum of the end face coincidence degree ε_α and the longitudinal coincidence degree ε_β. Considering

the environment and requirements of the planetary gearbox, the end face coincidence degree ε_α is $\varepsilon_\alpha \geq 1.3$, and the longitudinal coincidence degree ε_β is $\varepsilon_\beta \geq 1$. Therefore, the coincidence constraints in this paper are:

$$\begin{cases} c_{23}(\mathrm{X},\mathrm{X}^N,\mathrm{Y}^I,\mathrm{P}^N,\mathrm{P}^I) = 0.99 - P_{\mathrm{r\_worst}}\{g_{16}(\mathrm{X},\mathrm{X}^N,\mathrm{Y}^I,P^N,P^I) \leq 0\} \leq 0 \\ c_{24}(\mathrm{X},\mathrm{X}^N,\mathrm{Y}^I,\mathrm{P}^N,\mathrm{P}^I) = 0.99 - P_{\mathrm{r\_worst}}\{g_{17}(\mathrm{X},\mathrm{X}^N,\mathrm{Y}^I,P^N,P^I) \leq 0\} \leq 0 \\ c_{25}(\mathrm{X},\mathrm{X}^N,\mathrm{Y}^I,\mathrm{P}^N,\mathrm{P}^I) = 0.99 - P_{\mathrm{r\_worst}}\{g_{18}(\mathrm{X},\mathrm{X}^N,\mathrm{Y}^I,P^N,P^I) \leq 0\} \leq 0 \\ c_{26}(\mathrm{X},\mathrm{X}^N,\mathrm{Y}^I,\mathrm{P}^N,\mathrm{P}^I) = 0.99 - P_{\mathrm{r\_worst}}\{g_{19}(\mathrm{X},\mathrm{X}^N,\mathrm{Y}^I,P^N,P^I) \leq 0\} \leq 0 \\ c_{27}(\mathrm{X},\mathrm{X}^N,\mathrm{Y}^I,\mathrm{P}^N,\mathrm{P}^I) = 0.99 - P_{\mathrm{r\_worst}}\{g_{20}(\mathrm{X},\mathrm{X}^N,\mathrm{Y}^I,P^N,P^I) \leq 0\} \leq 0 \\ c_{28}(\mathrm{X},\mathrm{X}^N,\mathrm{Y}^I,\mathrm{P}^N,\mathrm{P}^I) = 0.99 - P_{\mathrm{r\_worst}}\{g_{21}(\mathrm{X},\mathrm{X}^N,\mathrm{Y}^I,P^N,P^I) \leq 0\} \leq 0 \end{cases} \tag{42}$$

$$g_{16}(\mathrm{X},\mathrm{X}^N,\mathrm{Y}^I,P^N,P^I) = 1.3 - \frac{1}{2\pi}[z_1(tan\,\alpha_{\mathrm{at1}} - tan\,2\,0^\circ) + z_2(tan\,\alpha_{\mathrm{at2}} - tan\,2\,0^\circ)] \tag{43}$$

$$z_2 = \frac{z_1}{2} \cdot \left(\frac{i_{45} \cdot i_{67}}{i} - 2\right) \tag{44}$$

$$g_{17}(\mathrm{X},\mathrm{X}^N,\mathrm{Y}^I,P^N,P^I) = 1.3 - \frac{1}{2\pi}[z_4(tan\,\alpha_{\mathrm{at4}} - tan\,2\,0^\circ) + z_5(tan\,\alpha_{\mathrm{at5}} - tan\,2\,0^\circ)] \tag{45}$$

$$z_5 = z_1 \cdot i_{45} \tag{46}$$

$$g_{18}(\mathrm{X},\mathrm{X}^N,\mathrm{Y}^I,P^N,P^I) = 1.3 - \frac{1}{2\pi}[z_6(tan\,\alpha_{\mathrm{at6}} - tan\,2\,0^\circ) + z_7(tan\,\alpha_{\mathrm{at7}} - tan\,2\,0^\circ)] \tag{47}$$

$$z_7 = z_6 \cdot i_{67} \tag{48}$$

where: $\alpha_{\mathrm{ati}}(i = 1\sim7)$ is the pressure angle of the tip circle of the intermeshing helical gears; i is the transmission ratio of the low-speed gear; g_{16}, g_{17} and g_{18} are the limit states of the end face coincidence of the three pairs of intermeshing helical gears.

$$g_{19}(\mathrm{X},\mathrm{X}^N,\mathrm{Y}^I,P^N,P^I) = 1 - \frac{b_1\,sin\,\beta_{123}}{\pi m_{\mathrm{n123}}} \tag{49}$$

$$b_1 = \frac{m_{\mathrm{n123}} z_1}{cos\,\beta_{123}} \cdot \phi_{\mathrm{d123}} \tag{50}$$

$$g_{20}(\mathrm{X},\mathrm{X}^N,\mathrm{Y}^I,P^N,P^I) = 1 - \frac{b_{45}\,sin\,\beta_{45}}{\pi m_{\mathrm{n45}}} \tag{51}$$

$$b_{45} = \frac{m_{\mathrm{n45}} z_4 \cdot i_{45}}{cos\,\beta_{45}} \cdot \phi_{\mathrm{d45}} \tag{52}$$

$$g_{21}(\mathrm{X},\mathrm{X}^N,\mathrm{Y}^I,P^N,P^I) = 1 - \frac{b_{67}\,sin\,\beta_{67}}{\pi m_{\mathrm{n67}}} \tag{53}$$

$$b_{67} = \frac{m_{\mathrm{n67}} z_6 \cdot i_{67}}{cos\,\beta_{67}} \cdot \phi_{\mathrm{d67}} \tag{54}$$

where: g_{19}, g_{20} and g_{21} are the limit states of longitudinal coincidence of three pairs of intermeshing helical gears.

Considering the transmission ratio, concentricity, assembly, and adjacency conditions comprehensively, the constraints of planetary gear transmission can be obtained:

$$c_{29}(\mathrm{X},\mathrm{X}^N,\mathrm{Y}^I,\mathrm{P}^N,\mathrm{P}^I) = 2 \cdot 1 - z_{1\_\mathrm{lower\_doundary}} \cdot \left[sin\frac{\pi}{3} - \frac{1}{2}\left(\frac{i_{45} \cdot i_{67}}{i} - 2\right) \cdot \left(1 - sin\frac{\pi}{3}\right)\right] \leq 0 \tag{55}$$

where: $z_{1\_\mathrm{lower\_doundary}}$ is the lower bound of the one-interval continuous design variable.

Considering the influence of parameters such as the circumferential force of the helical gear and the load of the planetary gear train, the constraint conditions for the contact fatigue strength of the helical gear tooth surface can be obtained as follows:

$$\begin{cases} c_{30}(\mathrm{X},\mathrm{X}^N,\mathrm{Y}^I,\mathrm{P}^N,\mathrm{P}^I) = 0.99 - Bel(Pr_{worst}\{g_{22}(X^N,\mathrm{Y}^I,P^N,P^I) \le 0\} - 0.99 > 0) \le 0 \\ c_{31}(\mathrm{X},\mathrm{X}^N,\mathrm{Y}^I,\mathrm{P}^N,\mathrm{P}^I) = 0.99 - Bel(Pr_{worst}\{g_{23}(X^N,\mathrm{Y}^I,P^N,P^I) \le 0\} - 0.99 > 0) \le 0 \\ c_{32}(\mathrm{X},\mathrm{X}^N,\mathrm{Y}^I,\mathrm{P}^N,\mathrm{P}^I) = 0.99 - Bel(Pr_{worst}\{g_{24}(X^N,\mathrm{Y}^I,P^N,P^I) \le 0\} - 0.99 > 0) \le 0 \\ c_{33}(\mathrm{X},\mathrm{X}^N,\mathrm{Y}^I,\mathrm{P}^N,\mathrm{P}^I) = 0.99 - Bel(Pr_{worst}\{g_{25}(X^N,\mathrm{Y}^I,P^N,P^I) \le 0\} - 0.99 > 0) \le 0 \end{cases} \tag{56}$$

$$g_{22}(X^N,\mathrm{Y}^I,P^N,P^I) = \sigma_{H2} - \sigma_{\mathrm{HP2}} \tag{57}$$

$$g_{23}(X^N,\mathrm{Y}^I,P^N,P^I) = \sigma_{H3} - \sigma_{\mathrm{HP3}} \tag{58}$$

$$g_{24}(X^N,\mathrm{Y}^I,P^N,P^I) = \sigma_{H4} - \sigma_{\mathrm{HP4}} \tag{59}$$

$$g_{25}(X^N,\mathrm{Y}^I,P^N,P^I) = \sigma_{H6} - \sigma_{\mathrm{HP6}} \tag{60}$$

Where: σ_{H2} and σ_{HP2} are the contact fatigue limit stress and allowable stress of the tooth surface of the planetary gear 2, respectively; σ_{H3} and σ_{HP3} are the contact fatigue limit stress and allowable stress of the tooth surface of the internal gear 3, respectively; σ_{Hi} and σ_{HPi} are the contact fatigue limit stress and allowable stress of the helical gear i, respectively (i=4, 6).

Considering the influence of the parameters such as the circumferential force of the helical gear and the load of the planetary gear train, the constraint condition of the bending fatigue strength of the root of the helical gear is:

$$\begin{cases} c_{34}(\mathrm{X},\mathrm{X}^N,\mathrm{Y}^I,\mathrm{P}^N,\mathrm{P}^I) = 0.99 - Bel(Pr_{worst}\{g_{26}(X^N,\mathrm{Y}^I,P^N,P^I) \le 0\} - 0.99 > 0) \le 0 \\ c_{35}(\mathrm{X},\mathrm{X}^N,\mathrm{Y}^I,\mathrm{P}^N,\mathrm{P}^I) = 0.99 - Bel(Pr_{worst}\{g_{27}(X^N,\mathrm{Y}^I,P^N,P^I) \le 0\} - 0.99 > 0) \le 0 \\ c_{36}(\mathrm{X},\mathrm{X}^N,\mathrm{Y}^I,\mathrm{P}^N,\mathrm{P}^I) = 0.99 - Bel(Pr_{worst}\{g_{28}(X^N,\mathrm{Y}^I,P^N,P^I) \le 0\} - 0.99 > 0) \le 0 \\ c_{37}(\mathrm{X},\mathrm{X}^N,\mathrm{Y}^I,\mathrm{P}^N,\mathrm{P}^I) = 0.99 - Bel(Pr_{worst}\{g_{29}(X^N,\mathrm{Y}^I,P^N,P^I) \le 0\} - 0.99 > 0) \le 0 \\ c_{38}(\mathrm{X},\mathrm{X}^N,\mathrm{Y}^I,\mathrm{P}^N,\mathrm{P}^I) = 0.99 - Bel(Pr_{worst}\{g_{30}(X^N,\mathrm{Y}^I,P^N,P^I) \le 0\} - 0.99 > 0) \le 0 \\ c_{39}(\mathrm{X},\mathrm{X}^N,\mathrm{Y}^I,\mathrm{P}^N,\mathrm{P}^I) = 0.99 - Bel(Pr_{worst}\{g_{31}(X^N,\mathrm{Y}^I,P^N,P^I) \le 0\} - 0.99 > 0) \le 0 \\ c_{40}(\mathrm{X},\mathrm{X}^N,\mathrm{Y}^I,\mathrm{P}^N,\mathrm{P}^I) = 0.99 - Bel(Pr_{worst}\{g_{32}(X^N,\mathrm{Y}^I,P^N,P^I) \le 0\} - 0.99 > 0) \le 0 \end{cases} \tag{61}$$

$$g_{26}(X^N,\mathrm{Y}^I,P^N,P^I) = \sigma_{\mathrm{F1}} - \sigma_{\mathrm{FP1}} \tag{62}$$

$$g_{27}(X^N,\mathrm{Y}^I,P^N,P^I) = \sigma_{\mathrm{F2}} - \sigma_{\mathrm{FP2}} \tag{63}$$

$$g_{28}(X^N,\mathrm{Y}^I,P^N,P^I) = \sigma_{\mathrm{F3}} - \sigma_{\mathrm{FP3}} \tag{64}$$

$$g_{29}(X^N,\mathrm{Y}^I,P^N,P^I) = \sigma_{\mathrm{F4}} - \sigma_{\mathrm{FP4}} \tag{65}$$

$$g_{30}(X^N,\mathrm{Y}^I,P^N,P^I) = \sigma_{\mathrm{F5}} - \sigma_{\mathrm{FP5}} \tag{66}$$

$$g_{31}(X^N,\mathrm{Y}^I,P^N,P^I) = \sigma_{\mathrm{F6}} - \sigma_{\mathrm{FP6}} \tag{67}$$

$$g_{32}(X^N,\mathrm{Y}^I,P^N,P^I) = \sigma_{\mathrm{F7}} - \sigma_{\mathrm{FP7}} \tag{68}$$

where: $\sigma_{\mathrm{F1}}$and σ_{FP1} are the bending fatigue limit stress and allowable stress of the tooth root of the sun gear 1, respectively; σ_{F2} and σ_{FP2} are the bending fatigue limit stress and allowable stress of the tooth root of the planetary gear 2; σ_{F3} and σ_{FP3} are the bending fatigue limit stress and allowable stress of the tooth root of the internal gear 3, respectively; σ_{Fi} and σ_{FPi} are the bending fatigue limit stress and allowable stress of the tooth root of the helical gear i respectively (i=4~7);

4.5. A Mathematical Model for EBDO Optimization Design of a Planetary Gearbox for 1.5MW Wind Turbine

Based on the above analysis and literature [28,30], there are 14 design variables and 40 constraints in this design, of which 32 are probabilistic constraints. The specific and complete mathematical model is:

$$
\begin{aligned}
\min_{\mathrm{X},\mathrm{X}^N,\mathrm{Y}^I} \quad & f=\frac{\pi}{4}\left(\frac{x_4x_1}{\cos x_7}\right)^3\cdot\left(\frac{x_{13}x_{14}}{i}-1\right)^2\cdot x_{10}+\frac{\pi}{4}\left(\frac{x_5x_2}{\cos x_8}\right)^3\cdot\left(1+x_{13}^2\right)\cdot x_{13}\cdot x_{11}\\
& +\frac{\pi}{4}\left(\frac{x_6x_3}{\cos x_9}\right)^3\cdot\left(1+x_{14}^2\right)\cdot x_{14}\cdot x_{12}\\
\text{s.t.}\ \ & c_{1\sim3}\left(\mathrm{X},\mathrm{X}^N,\mathrm{Y}^I,\mathrm{P}^N,\mathrm{P}^I\right)=0.99-\mathrm{Pr\_worst}\left\{g_{1\sim3}\left(\mathrm{X},\mathrm{X}^N,\mathrm{Y}^I,\mathrm{P}^N,\mathrm{P}^I\right)\le0\right\}\le0\\
& c_4\left(\mathrm{X},\mathrm{X}^N,\mathrm{Y}^I,\mathrm{P}^N,\mathrm{P}^I\right)=2-m_{\mathrm{n123}}\le0\\
& c_5\left(\mathrm{X},\mathrm{X}^N,\mathrm{Y}^I,\mathrm{P}^N,\mathrm{P}^I\right)=2-m_{\mathrm{n45}}\le0\\
& c_6\left(\mathrm{X},\mathrm{X}^N,\mathrm{Y}^I,\mathrm{P}^N,\mathrm{P}^I\right)=2-m_{\mathrm{n67}}\le0\\
& c_{7\sim12}\left(\mathrm{X},\mathrm{X}^N,\mathrm{Y}^I,\mathrm{P}^N,\mathrm{P}^I\right)=0.99-\mathrm{P_r}\left\{g_{4\sim9}\left(\mathrm{X},\mathrm{X}^N,\mathrm{Y}^I,\mathrm{P}^N,\mathrm{P}^I\right)\le0\right\}\le0\\
& c_{13}\left(\mathrm{X},\mathrm{X}^N,\mathrm{Y}^I,\mathrm{P}^N,\mathrm{P}^I\right)=1.01i_{45}-i_{67}\le0\\
& c_{14}\left(\mathrm{X},\mathrm{X}^N,\mathrm{Y}^I,\mathrm{P}^N,\mathrm{P}^I\right)=i_{67}-1.05i_{45}\le0\\
& c_{15}\left(\mathrm{X},\mathrm{X}^N,\mathrm{Y}^I,\mathrm{P}^N,\mathrm{P}^I\right)=1/9-i/\left(i_{45}\cdot i_{67}\right)\le0\\
& c_{16}\left(\mathrm{X},\mathrm{X}^N,\mathrm{Y}^I,\mathrm{P}^N,\mathrm{P}^I\right)=i/\left(i_{45}\cdot i_{67}\right)-1/2.7\le0\\
& c_{17\sim22}\left(\mathrm{X},\mathrm{X}^N,\mathrm{Y}^I,\mathrm{P}^N,\mathrm{P}^I\right)=0.99-\mathrm{P_r}\left\{g_{10\sim15}\left(\mathrm{X},\mathrm{X}^N,\mathrm{Y}^I,\mathrm{P}^N,\mathrm{P}^I\right)\le0\right\}\le0\\
& c_{29}\left(\mathrm{X},\mathrm{X}^N,\mathrm{Y}^I,\mathrm{P}^N,\mathrm{P}^I\right)=2\cdot1-z_{1\_\mathrm{lower\_doundary}}\cdot\left[\begin{array}{l}\sin\dfrac{\pi}{3}-\\ \dfrac{1}{2}\left(\dfrac{i_{45}\cdot i_{67}}{i}-2\right)\cdot\left(1-\sin\dfrac{\pi}{3}\right)\end{array}\right]\le0\\
& c_{30\sim40}\left(\mathrm{X},\mathrm{X}^N,\mathrm{Y}^I,\mathrm{P}^N,\mathrm{P}^I\right)=0.99-Bel\left(\mathrm{Pr}_{worst}\left\{g_{22\sim32}\left(\begin{array}{l}\mathrm{X}^N,\mathrm{Y}^I,\\ \mathrm{P}^N,\mathrm{P}^I\end{array}\right)\le0\right\}-0.99>0\right)\le0
\end{aligned}
\tag{69}
$$

where: the constraints with the same representation form are combined and described together. For example, $c_{1\sim3}(\mathrm{X},\mathrm{X}^N,\mathrm{Y}^I,\mathrm{P}^N,\mathrm{P}^I)$ represents 1, 2, 3 of the constraint condition, and $g_{1\sim3}(\mathrm{X},\mathrm{X}^N,\mathrm{Y}^I,P^N,P^I)$ represents 1, 2, 3 of the limit state function.

5. Optimization of EBDO and analysis of results

The mathematical model built in the fourth part is solved by MATLAB. The obtained results are shown in Tables **1**-**3**.

Table 1: Volume optimization results

	Optimization Results	Rounded results	Initial data
V(mm^3)	7.9407×10^8	6.7439×10^8	8.0146×10^8

Analyzed by volume: For the convenience of calculation, it is assumed that the number of teeth and the module are continuous design variables, and the limit conditions are constraints. Rounding to a small direction or to a large direction during rounding has no effect on the Bel and Pl of the corresponding limit state function. To

minimize the design objective, the number of teeth and the module are rounded toward the small boundary during rounding. In this way, the rounded data can satisfy the constraints and reduce the design goals.

Only from the volume analysis of the design target: the volume of the optimized planetary gearbox is $7.9407 \times 10^8 \text{mm}^3$; the calculated volume after all data is rounded is $6.7439 \times 10^8 \text{mm}^3$. This is 15.85% less than the original volume of planetary gearbox $8.0146 \times 10^8 \text{mm}^3$.

Table 2: Comparison of gear tooth surface contact fatigue strength and tooth root bending fatigue strength reliability before and after rounding.

		Before Rounding [*Bel-Pl*]	After Rounding [*Bel-Pl*]
Contact fatigue strength reliability of tooth surface	Meshing of wheel 1 and 2	[0.9998-0.9999]	[0.9998-0.9999]
	Meshing of wheel 2 and 3	[1.0000-1.0000]	[1.0000-1.0000]
	Meshing of wheel 4 and 6	[0.9910-0.9977]	[0.9910-0.9977]
	Meshing of wheel 6 and 7	[0.9998-0.9999]	[0.9998-0.9999]
Reliability of tooth root bending fatigue strength	Sun gear 1	[0.9999-1.0000]	[0.9999-1.0000]
	Planetary gear 2	[0.9913-0.9949]	[0.9913-0.9949]
	Ring gear 3	[0.9999-1.0000]	[0.9999-1.0000]
	Helical gear 4	[0.9959-0.9999]	[0.9959-0.9999]
	Helical gear 5	[0.9986-0.9999]	[0.9986-0.9999]
	Helical gear 6	[1.0000-1.0000]	[1.0000-1.0000]
	Helical gear 7	[0.9999-1.0000]	[0.9999-1.0000]

Analysis from the degree of confidence: the reliability of the contact fatigue strength of the large gears in each meshing gear pair in the planetary gearbox and the reliability of the bending fatigue strength of the tooth roots of each helical gear is between the degree of confidence and the degree of likelihood, namely:

$$Bel(g_i) \le Pr(g_i) \le Pl(g_i), \quad i = 22 \sim 32 \tag{70}$$

The Bel and Pl of gear contact fatigue strength and tooth root bending fatigue strength did not change before and after the optimization results. This is also the result of considering the number of gear teeth and the modulus as a single interval link variable in the design. The reliability of the contact fatigue strength of each meshing gear pair in the planetary gearbox and the reliability of the tooth root bending fatigue strength of each helical gear are above 0.99. This all meets the design requirements.

Table 3: Coincidence comparison of meshing gear pairs.

Meshing Gear Pair	End Face Coincidence		Axial Coincidence	
	Original Value	Design Value	Original Value	Design Value
Wheel 1- Wheel 2	1.3459	1.7261	1.2782	1.5103
Wheel 2- Wheel 3	1.5942	1.7983	1.2749	1.5057
Wheel 4- Wheel 5	1.4549	1.6982	1.2441	1.6913
Wheel 6- Wheel 7	1.5340	1.6969	1.4411	1.7799

Analysis from the coincidence degree of meshing gear pairs: This design improves the end face coincidence and axial coincidence of each meshing gear pair. This increases the transmission stability of the wind turbine speed increaser and improves the bearing capacity of the helical gear.

The optimized volume results of the proposed method and Sequence Optimization and Reliability Assess (SORA), which only considers random uncertainty, are shown in Table **4**:

Table 4: The proposed method and SORA optimization results.

	Volume before Optimization (mm3)	Optimized Volume (mm3)	Volume Reduction Rate
The proposed method	8.0146×10^8	6.7439×10^8	15.85%
SORA	8.0146×10^8	6.8041×10^8	15.10%

Table **4** shows that the optimization effect of the proposed method is better than SORA. Moreover, the proposed method considers the influence of subjective uncertainty, which makes the optimization results of the proposed method safer.

Based on the above analysis: It is feasible and effective to adopt the EBDO optimization design considering interval variables and random variables for the planetary gearbox of the megawatt wind turbine.

6. Conclusion

In this paper, the EBDO, which only considers interval variables, is improved. Furthermore, both interval variables and random variables are considered in the optimization design process. Then, taking the optimal design of the planetary gearbox for a megawatt wind turbine as the research object, the uncertainty factors in the optimal design of the wind turbine planetary gearbox are analyzed. On this basis, the proposed method is used to optimize the design of the planetary gearbox. The final comparative analysis shows the result of planetary gearbox optimization, and the optimization design scheme of this paper is feasible.

Acknowledgments

The support from the Sichuan Science and Technology Program (Grant No. 2022YFQ0087) and the Sichuan Science and Technology Innovation Seedling Project Funding Project (Grant No. 2021112) are gratefully acknowledged.

References

[1] Qian G. Overview of hydro-wind-solar power complementation development in China. Global Energy Interconnection, 2019; 2(4): 285-289. https://doi.org/10.1016/j.gloei.2019.11.011

[2] Wang T, Han Q, Chu F, Feng Z. Vibration based condition monitoring and fault diagnosis of wind turbine planetary gearbox: A review. Mechanical Systems and Signal Processing, 2019; 126: 662-685. https://doi.org/10.1016/j.ymssp.2019.02.051

[3] Li G, Liu W, Su X. The Sun and Planetary Gear Design of a 1.5-MW Wind Turbine. Journal of Vibration Engineering & Technologies, 2018; 6(6): 495-501. https://doi.org/10.1007/s42417-018-0066-8

[4] Yang Y, Li H, Yao J, Gao W, Peng H. Analysis on the force and life of gearbox in double-rotor wind turbine. Energies, 2019; 12(21): 4220. https://doi.org/10.3390/en12214220

[5] Chen X, Yang X, Zuo MJ, Tian Z. Planetary gearbox dynamic modeling considering bearing clearance and sun gear tooth crack. Sensors, 2021; 21(8): 2638. https://doi.org/10.3390/s21082638

[6] Hazbavi Z, Baartman JE, Nunes JP, Keesstra SD, Sadeghi SH. Changeability of reliability, resilience and vulnerability indicators with respect to drought patterns. Ecological Indicators, 2018; 87: 196-208. https://doi.org/10.1016/j.ecolind.2017.12.054

[7] Monsef H, Naghashzadegan M, Farmani R, Jamali A. Deficiency of reliability indicators in water distribution networks. Journal of Water Resources Planning and Management, 2019; 145(6): 04019022. https://doi.org/10.1061/(ASCE)WR.1943-5452.0001053

[8] Meng D, Lv Z, Yang S, Wang H, Xie T, Wang Z. A time-varying mechanical structure reliability analysis method based on performance degradation. Structures, 2021; 34: 3247-3256. https://doi.org/10.1016/j.istruc.2021.09.085

[9] Abd Rahim AA, Abdullah S, Singh SSK, Nuawi MZ. Reliability assessment on automobile suspension system using wavelet analysis. International Journal of Structural Integrity, 2019; 10(5): 602-611. https://doi.org/10.1108/IJSI-04-2019-0035

[10] Yang YJ, Wang G, Zhong Q, Zhang H, He J, Chen H. Reliability analysis of gas pipeline with corrosion defect based on finite element method. International Journal of Structural Integrity, 2021; 12(6): 854-863. https://doi.org/10.1108/IJSI-11-2020-0112

[11] Xi, Z. Model-based reliability analysis with both model uncertainty and parameter uncertainty. Journal of Mechanical Design, 2019; 141(5): 051404. https://doi.org/10.1115/1.4041946

[12] Schietzold FN, Leichsenring F, Götz M, Graf W, Kaliske M. Robustness versus Performance-Nested Inherence of Objectives in Optimization with Polymorphic Uncertain Parameters. Advances in Engineering Software, 2021; 156: 102932. https://doi.org/10.1016/j.advengsoft.2020.102932

[13] Ding S. Uncertain random quadratic bottleneck assignment problem. Journal of Ambient Intelligence and Humanized Computing, 2020; 11(8): 3259-3264. https://doi.org/10.1007/s12652-019-01510-z

[14] Mourelatos ZP, Zhou J. A design optimization method using evidence theory. Journal of Mechanical Design, 2005; 128(4): 901-908. https://doi.org/10.1115/1.2204970

[15] Keshtegar B, Seghier MEAB, Zhu SP, Abbassi R, Trung NT. Reliability analysis of corroded pipelines: Novel adaptive conjugate first order reliability method. Journal of Loss Prevention in the Process Industries, 2019; 62: 103986. https://doi.org/10.1016/j.jlp.2019.103986

[16] Al-Ani A, Deriche M. A new technique for combining multiple classifiers using the Dempster-Shafer theory of evidence. Journal of Artificial Intelligence Research, 2002; 17: 333-361. https://doi.org/10.1613/jair.1026

[17] Zhang J, Xiao M, Gao L, Qiu H, Yang Z. An improved two-stage framework of evidence-based design optimization. Structural and Multidisciplinary Optimization, 2018; 58(4): 1673-1693. https://doi.org/10.1007/s00158-018-1991-6

[18] Han Y, Liu S, Geng Z, Gu H, Qu Y. Energy analysis and resources optimization of complex chemical processes: Evidence based on novel DEA cross-model. Energy, 2021; 218: 119508. https://doi.org/10.1016/j.energy.2020.119508

[19] Liu P, Liu X, Ma G, Liang Z, Wang C, Alsaadi FE. A multi-attribute group decision-making method based on linguistic intuitionistic fuzzy numbers and Dempster-Shafer evidence theory. International Journal of Information Technology & Decision Making, 2020; 19(02): 499-524. https://doi.org/10.1142/S0219622020500042

[20] Du YW, Zhong JJ. Generalized combination rule for evidential reasoning approach and Dempster-Shafer theory of evidence. Information Sciences, 2021; 547: 1201-1232. https://doi.org/10.1016/j.ins.2020.07.072

[21] Meng Z, Guo L, Wang X. A general fidelity transformation framework for reliability-based design optimization with arbitrary precision. Structural and Multidisciplinary Optimization, 2022; 65(1): 1-16. https://doi.org/10.1007/s00158-021-03091-y

[22] Montonen J, Nerg J, Polikarpova M, Pyrhönen J. Integration principles and thermal analysis of an oil-cooled and-lubricated permanent magnet motor planetary gearbox drive system. IEEE Access, 2019; 7: 69108-69118. https://doi.org/10.1109/ACCESS.2019.2919506

[23] Yuan R, Li H, Wang Q. An enhanced genetic algorithm-based multi-objective design optimization strategy. Advances in Mechanical Engineering, 2018; 10(7): 1687814018784836. https://doi.org/10.1177/1687814018784836

[24] Vlami V, Danek J, Zogaris S, Gallou E, Kokkoris IP, Kehayias G, Dimopoulos P. Residents' Views on Landscape and Ecosystem Services during a Wind Farm Proposal in an Island Protected Area. Sustainability, 2020; 12(6): 2442. https://doi.org/10.3390/su12062442

[25] Keshavarzzadeh V, Ghanem RG, Tortorelli D. A. Shape optimization under uncertainty for rotor blades of horizontal axis wind turbines. Computer Methods in Applied Mechanics and Engineering, 2019; 354: 271-306. https://doi.org/10.1016/j.cma.2019.05.015

[26] Ding F, Tian,Z. Integrated Prognosis for Wind Turbine Gearbox Condition-Based Maintenance Considering Time-Varying Load and Crack Initiation Time Uncertainty. International Journal of Reliability, Quality and Safety Engineering, 2021; 28(04): 2150024. https://doi.org/10.1142/S0218539321500248

[27] Behera SK, Meena H, Chakraborty S, Meikap BC. Application of response surface methodology (RSM) for optimization of leaching parameters for ash reduction from low-grade coal. International Journal of Mining Science and Technology, 2018; 28(4): 621-629. https://doi.org/10.1016/j.ijmst.2018.04.014

[28] Guiling H. Reliability Optimization Design of Transmission Mechanism of Automobile Mechanical Transmission Based on Feature Extraction. Solid State Technology, 2020; 63(4): 8603-8611.

[29] Yingcheng X, Nengling T. Review of contribution to frequency control through variable speed wind turbine. Renewable energy, 2011; 36(6): 1671-1677. https://doi.org/10.1016/j.renene.2010.11.009

[30] Lu L, He Y, Ruan Y, Yuan W. Wind turbine planetary gearbox condition monitoring method based on wireless sensor and deep learning approach. IEEE Transactions on Instrumentation and Measurement, 2020; 70: 1-16. https://doi.org/10.1109/TIM.2021.3118092